濟大論文集(自然), 38, 343-348, 1994
Cheju Univ. Jour. (Natural Sci.),
38, 343-348, 1994

Analysis for ^{6}Li Ion Elastic Scattering by Using Nuclear-Modified Glauber Model

Yong-Joo Kim, Sung-Rak Hong**

핵-수정된 Glauber 모형을 이용한 ^{6}Li이온의 탄성산란에 대한 분석

김용주*, 홍성락*

Summary

Using the nuclear-modified Glauber model by taking into account the classical perturbation of Coulomb trajectory due to the nuclear potential, the elastic scattering angular distributions of heavy ions are examined. This model has been applied satisfactorily to elastic scatterings of the systems ^{6}Li+^{40}Ca and ^{6}Li+^{90}Zr at E_{lab}=210 MeV. The near-side and far-side decompositions of elastic cross sections following the Fuller formalism have been also performed.

Introduction

In recent years, much interest is being focused on heavy ion elastic scattering. One of the methods for the analysis of elastic scattering data is the optical limit to the Glauber theory (Chauvin et al., 1983; Chauvin et al., 1985; Vitturi and Zardi, 1987; Charagi and Gupta, 1990; Charagi and Gupta, 1992). This method of analysis has been quite successful in describing the heavy ion elastic scattering.

In the simple Glauber approach to heavy ion elastic scattering (Chauvin et al., 1983; Chauvin et al., 1985), it is assumed that the flux attenuation of the elastic channel occurs by means of nucleon-nucleon collisions along a classical straight-line trajectory. Vitturi and Zardi (1987) modified the standard form of Glauber model to account for the Coulomb distortion of the trajectories occurring in the case of heavy ion scattering and applied it successfully to elastic scattering for E_{lab}=1760 MeV ^{40}Ar and 390 MeV ^{12}C ions on ^{208}Pb target nuclei. Such a model is known as the Coulomb-modified Glauber model (CGM).

* 자연과학대학 물리학과(Dept. of Physics, Cheju Univ., Cheju-do, 690-756, Korea)

In the previous papers (Cha and Kim, 1992; Cha et al., 1993), we have presented a nuclear-modified Glauber model for describing elastic and inelastic scattering processes between heavy ions. This model is included the deflection effects due to the Coulomb and real nuclear potential, to first order, in the manner of Brink and Satchler (1981), in which it has been taken into account the change in turning point due to nuclear potential by expanding E-V(r) about $r=d_0$.

Another approach to include the deflection effect of heavy-ion trajectory due to nuclear potential has been found from classical perturbation of Coulomb trajectory by Christensen and Winther (1976). Some years ago, Nadasen et al. (1989) have observed the elastic scattering angular distributions for ^{6}Li on ^{40}Ca and ^{90}Zr at $E_{lab}=210$ MeV and have analyzed these data using the optical model. In this paper, we analyze the ^{6}Li+^{40}Ca and ^{6}Li+^{90}Zr elastic scattering at $E_{lab}=210$ MeV based on the nuclear-modified Glauber model (NGM) by taking into account the classical perturbation of the Coulomb trajectory due to relatively weak nuclear potential in addition to Coulomb field of the Coulomb-modified Glauber model. In Sec. Ⅱ, we present the scattering amplitude in the nuclear-modified Glauber model. Results and conclusions are presented in Sec. Ⅲ.

Scattering Amplitude in the NGM

The differential cross section for the elastic scattering is given by the following equation :

$$\frac{d\sigma}{d\Omega} = |f(\theta)|^2 \qquad (1)$$

where the elastic scattering amplitude $f(\theta)$ for spin-zero particle via Coulomb and short range central forces can be separated into the Rutherford and nuclear parts by writing (Brink, 1985)

$$f(\theta) = f_R(\theta) + \frac{1}{ik}\sum_{\ell=0}^{\infty} (\ell+\tfrac{1}{2}) \exp(2i\sigma_\ell) (S_\ell^N - 1) P_\ell(\cos\theta). \qquad (2)$$

Here, $f_R(\theta)$ is the usual Rutherford scattering amplitude, $\sigma_\ell = \arg\Gamma(\ell+1+i\eta)$ are the Coulomb phase shifts and $\eta = mZ_1Z_2e^2/(\hbar^2k)$ is the Sommerfeld parameter.

In the standard Glauber model optical limit, the nuclear scattering matrix S_ℓ^N is expressed as (Chauvin et al., 1983)

$$S_\ell^N = \exp\{\frac{2\pi i}{k_{NN}} \Omega_\ell f_{NN}(0)\}, \qquad (3)$$

where the scattering amplitude for the nucleon-nucleon scattering at $\theta=0^\circ$, $f_{NN}(0)$, is related to the average nucleon-nucleon total cross section σ_{NN} through

$$f_{NN}(0) = \frac{k_{NN}}{4\pi} \sigma_{NN}(\alpha_{NN}+i), \qquad (4)$$

where α_{NN} is the ratio of the real to the imaginary part of the forward nucleon-nucleon scattering amplitude. In determining the value of σ_{NN}, it is convenient to use the expressions given by the Charagi and Gupta (1990). Ω_ℓ is the overlap integral of the nuclear densities along a straight line trajectory characterized by the impact parameter $b=(\ell+\frac{1}{2})/k$. In the Coulomb-modified Glauber model, the impact parameter b is replaced by the distance of closest approach, d_0 :

$$d_0 = \frac{1}{k}[\eta + (\eta^2 + (\ell+\tfrac{1}{2})^2)^{1/2}]. \qquad (5)$$

Assuming a Gaussian distribution of the nuclear density (Chauvin et al., 1983; Vitturi and Zardi, 1987)

$$\rho_i(r) = \rho_i(0) \exp(-r^2/a_i^2) \quad (i=T, P) \qquad (6)$$

for both target and projectile, Ω_ℓ is given by

$$\Omega_\ell = \rho_P(0)\,\rho_T(0)\,\pi^2 \frac{a_P^3 a_T^3}{a_P^2+a_T^2} \exp\left(\frac{-d_0^2}{a_P^2+a_T^2}\right) , \quad (7)$$

where a_i and $\rho_i(0)$ are usually determined from the experimental RMS radii.

Equation (5) assumes point charges interacting via the Coulomb field alone. It therefore does not include the deflection in the trajectory of heavy ion due to the real nuclear potential. As is shown Christensen and Winther (1976), the deflection effects due to the Coulomb and relatively weak nuclear potentials are determined by the classical perturbation theory.

In the first order perturbation theory, one can find that the distance of closest approach is given by (Christensen and Winther, 1976)

$$d = d_0 + \Delta \quad (8)$$

with

$$\Delta = d_0 \frac{1+\epsilon_\ell}{\epsilon_0} \frac{V_N(d_0)}{2E} , \quad (9)$$

where ϵ_ℓ is the eccentricity in the hyperbolic orbit

$$\epsilon_\ell = \left[1+\left(\frac{\ell+\frac{1}{2}}{\eta}\right)^2\right]^{1/2} \quad (10)$$

and $V_N(d_0)$ is the nuclear potential in the form

$$V_N(d_0) = -\frac{V_0}{1+e^{(d_0-R)/a}} . \quad (11)$$

In the nuclear-modified Glauber model with classical perturbation of the Coulomb trajectory, the distance of closest approach d_0 is replaced by d given in Eq. (8).

Results and Conclusions

We have applied the nuclear-modified Glauber model formalism to the elastic scatterings of ^{6}Li+^{40}Ca and ^{6}Li+^{90}Zr at E_{lab}=210 MeV. Table 1 shows the input values in the NGM and in the CGM to calculate the differential cross sections. In Figs. 1(a) and 1(b), the broken curves represent the cross sections obtained in the CGM optical limits and the solid curves denote the results in our NGM optical limit. It is seen that the agreement of the our NGM results with the experimental values (Nadasen et al., 1989) is remarkably good with respect to the results of the CGM. We can see in Table 1 that values of χ^2/N apparently decrease in the NGM compared with the results in CGM.

In Fig. 2, we plot curves of the transmission function $T_\ell = 1-|S_\ell^N|^2$ for the elastic scatterings of ^{6}Li+^{40}Ca and ^{6}Li+^{90}Zr at E_{lab}=210 MeV. Solid and broken curves, in Fig. 2, denote the transmission functions calculated by NGM and CGM, respectively. It is noted that the broken curves are undistinguishable from the solid ones. As seen in table 1, such facts are reflected in the

Table 1. Input values and total reaction cross sections (σ_R) in the Coulomb-modified Glauber model (CGM) and nuclear-modified Glauber model (NGM) for ^{6}Li+^{40}Ca and ^{6}Li+^{90}Zr at E_{lab}=210 MeV. The RMS radius are taken from Charagi and Gupta (1990).

Target	σ_{NN}^a (mb)	α_{NN}	V_0 (MeV)	r_0 (fm)	a (fm)	CGM σ_R (mb)	NGM σ_R (mb)	CGM χ^{2b}/N	NGM χ^{2b}/N
^{40}Ca	165.4	0.775	20	1.06	0.26	1889.9	1890.4	24.9	16.9
^{90}Zr	165.4	0.751	20	1.10	0.22	2675.7	2676.0	30.3	19.1

[a] σ_{NN} are obtained by using equations (22) and (23) in Charagi and Gupta (1990), instead of experimental values.

[b] 10% error bars

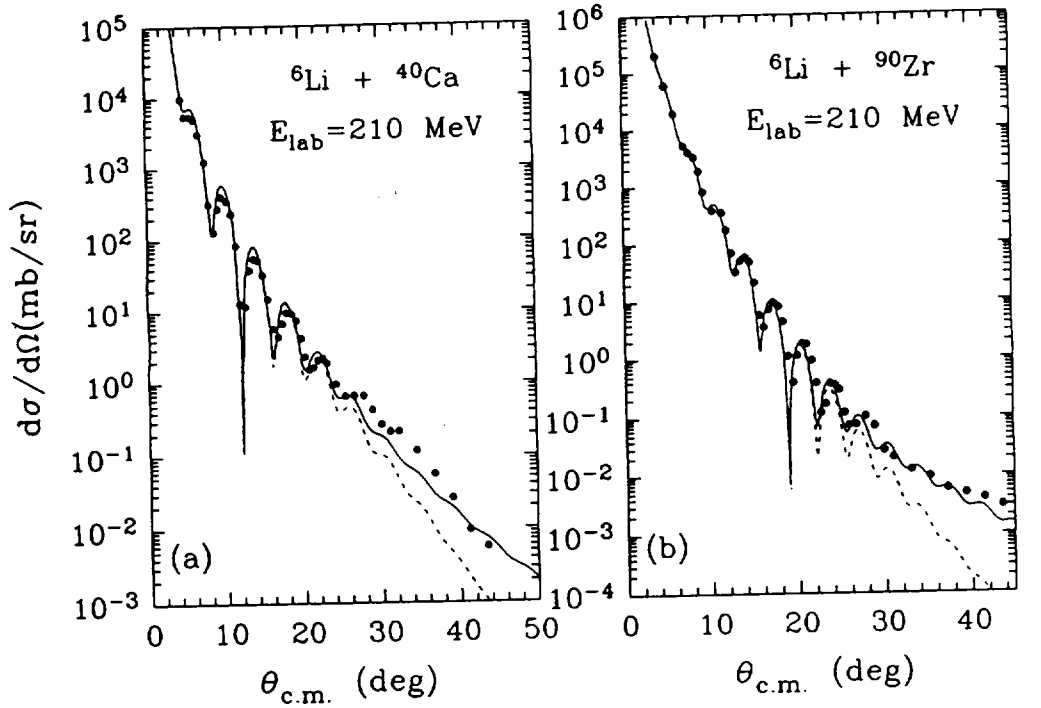

Fig. 1. Elastic scattering angular distributions for systems (a) ^{6}Li+^{40}Ca and (b) ^{6}Li+^{90}Zr at E_{lab}= 210 MeV. The solid circles denote the observed data taken from Nadasen et al. (1989). Solid and broken curves are the calculated results from the nuclear-modified Glauber model and the Coulomb-modified Glauber model, respectively.

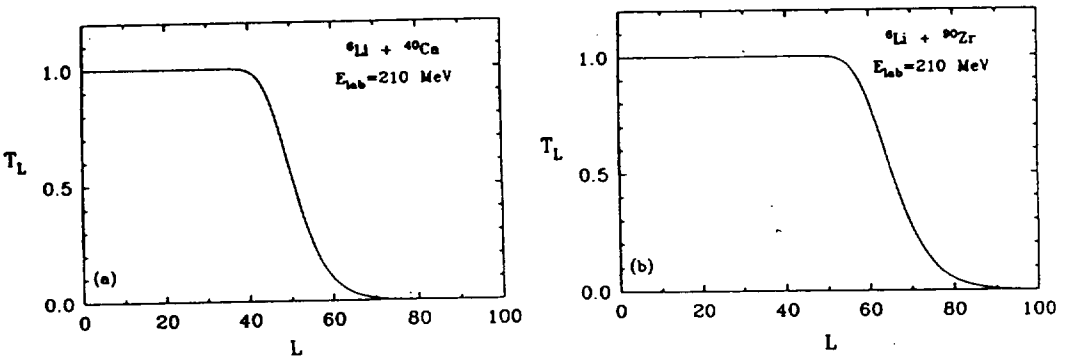

Fig. 2. Transmission functions for (a) ^{6}Li+^{40}Ca and (b) ^{6}Li+^{90}Zr systems at E_{lab}=210 MeV plotted versus the orbital angular momentum. Solid and broken curves are the calculated results from nuclear-modified Glauber model and Coulomb-modified Glauber model, respectively. Here the broken curves are undistinguishable from the solid ones.

total reaction cross sections. In the elastic scatterings of ^{6}Li+^{40}Ca and ^{6}Li+^{90}Zr at E_{lab}=210 MeV, the total reaction cross sections calculated by NGM are a little larger than ones by CGM. We can see also that transmission functions are shifted to the right as the target mass increases,

in this figure.

The near- and far-side decompositions of the scattering amplitudes were also performed by following the Fuller's formalism (Fuller, 1975). The contributions of the near- and far-side components to elastic scattering cross sections for the systems ^{6}Li+^{40}Ca and ^{6}Li+^{90}Zr at E_{lab}= 210 MeV are shown in Fig. 3 along with the total differential cross sections. The total differential cross sections is not just a sum of the near- and far-side cross sections, but contains the interference between near- and far-side components. The oscillations observed on the elastic angular distributions of ^{6}Li+^{40}Ca and ^{6}Li+^{90}Zr are both due to the strong interferences between the near- and far-side components. The magnitudes of the near- and far-side contributions are about the same at $\theta_{c.m.}=12.2°$ for ^{6}Li+^{40}Ca and at $\theta_{c.m.}=18.8°$ for ^{6}Li+^{90}Zr, respectively. However, the far-side contributions to the cross sections dominate both at the regions greater than those angles.

In this paper, we have presented a nuclear-modified Glauber model for heavy ion elastic scattering to take into account the deflection effect in the trajectory due to the relatively weak nuclear potential in addition to the Coulomb effect in the Coulomb-modified Glauber model. It has been applied satisfactorily to the elastic scatterings of ^{6}Li+^{40}Ca and ^{6}Li+^{90}Zr at E_{lab}=210 MeV. We can see that the oscillations observed on the elastic angluar distributions of ^{6}Li+^{40}Ca and ^{6}Li+^{90}Zr have been understood due to the strong interferences between the near- and far-side amplitudes.

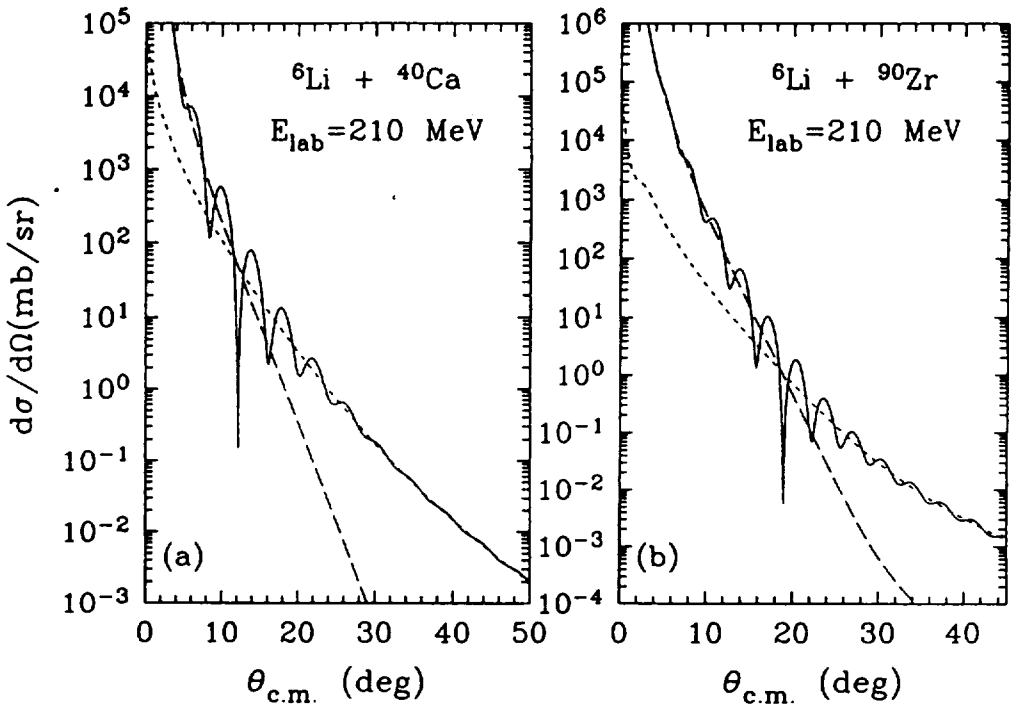

Fig. 3. Differential cross sections (solid curves), near-side contributions (long-dashed curves) and far-side contributions (short-dashed curves) following the Fuller's formalism (Fuller, 1975) by using the nuclear-modified Glauber model for the systems (a) ^{6}Li+^{40}Ca and (b) ^{6}Li+^{90}Zr at E_{lab}=210 MeV.

References

Brink D. M., 1985. *Semi-classical methods for the nucleus-nucleus scattering* (Cambridge Univ. Press, Cambridge), pp. 12-13.

Brink D. M. and G. R. Satchler, 1981. The role of the attractive nuclear potential in determining reaction cross sections, J. Phys. G7, 43-52.

Cha M. H. and Y. J. Kim, 1992. Modified Glauber-model description for $^{12}C+^{12}C$ elastic scattering, J. Phys. G18, L183-L186.

Cha M. H., B. K. Lee, Y. J. Kim and M. W. Kim, 1993. Nuclear-Modified Glauber Model Description for Heavy-Ion Inelastic Scattering, J. Korean Phys. Soc. 26, 451-454.

Charagi S. K. and S. K. Gupta, 1990. Coulomb-modified Glauber model description of heavy-ion reaction cross sections, Phys. Rev. C41, 1610-1618.

Charagi S. K. and S. K. Gupta, 1992. Coulomb-modified Glauber model description of heavy-ion elastic scattering at low energies. Phys. Rev. C46, 1982-1987.

Chauvin J., D. Lebrun, A. Lounis, and M. Buenerd, 1983. Low and intermediate energy nucleus-nucleus elastic scattering and the optical limit of Glauber theory, Phys. Rev. C28, 1970-1974.

Chauvin J., D. Lebrun, F. Durand, and M. Buenerd, 1985. Inelastic $^{12}C(^{12}C, ^{12}C)$ ^{12}C scattering via the Glauber optical potential at E/A=30 MeV and 85 MeV, J. Phys. G11, 261-266.

Christensen P. R. and A. Winther, 1976. The evidence on the ion-ion potentials from heavy ion elastic scattering, Phys. Lett. 65B, 19-22.

Fuller R. C., 1975. Qualitative behavior of heavy-ion elastic scattering angular distributions, Phys. Rev. C12, 1561-1574.

Nadasen A., M. McMaster, M. Fingal, J. Tavormina, P. Schwandt, J. S. Winfield, M. F. Mohar, F. D. Becchetti, J. W. Janecke and R. E. Warner, 1989. Unique ^{6}Li-nucleus optical potentials from elastic scattering of 210 MeV ^{6}Li ions by ^{28}Si, ^{40}Ca, ^{90}Zr, and ^{208}Pb, Phys. Rev. C39, 536-545.

Vitturi A. and F. Zardi, 1987. Modified Glauber model for the description of elastic scattering between heavy ions, Phys. Rev. C36, 1404-1407.

〈국문초록〉

핵-수정된 Glauber 모형을 이용한 ^{6}Li이온의 탄성산란에 대한 분석

핵 피텐셜에 기인한 쿨롱궤도의 고전적 섭동론이 고려된 핵-수정된 Glauber 모형을 이용하여 중이온 탄성산란의 각분포를 조사하였다. 이 모형은 E_{lab}=210 MeV인 $^{6}Li+^{40}Ca$와 $^{6}Li+^{90}Zr$계의 탄성산란에 성공적으로 적용될 수 있었다. Fuller 포말리즘을 이용한 탄성산란 단면적의 근측, 원측 분해도 역시 수행되었다.